

TWO-DIMENSIONAL FLUIDS VIA MATRIX HYDRODYNAMICS

KLAS MODIN¹ AND MILO VIVIANI²

ABSTRACT. Two-dimensional (2-D) incompressible, inviscid fluids produce fascinating patterns of swirling motion. How and why the patterns emerge are long-standing questions, first addressed in the 19th century by Helmholtz, Kirchhoff, and Kelvin. Countless researchers have since contributed to innovative techniques and results, but the overarching problem of swirling 2-D motion and its long-time behavior remains largely open. Here we advocate an alternative view-point that sheds light on this problem via a link to isospectral matrix flows. The link is established through V. Zeitlin’s beautiful model for the numerical discretization of Euler’s equations in 2-D. When considered on the sphere, Zeitlin’s model enables a deep connection between 2-D hydrodynamics and unitary representation theory of Lie algebras as pursued in quantum theory. Consequently, it provides a dictionary that maps hydrodynamical concepts to matrix Lie theory, which in turn gives connections to matrix factorizations, random matrices, and integrability theory, for example. The transfer of outcomes, from finite-dimensional matrices to infinite-dimensional fluids, is then supported by hard-fought results in quantization theory – the field which describes the limit between quantum and classical physics. We demonstrate how the dictionary is constructed and how it unveils techniques for 2-D hydrodynamics. We also give accompanying convergence results for Zeitlin’s model on the sphere.

CONTENTS

| | |
|---|----|
| 1. Introduction | 2 |
| 2. Background: geometry of the 2-D Euler equations | 4 |
| 3. Quantization and the Euler–Zeitlin equation | 6 |
| 3.1. Quantization via representation | 7 |
| 4. Coadjoint orbits and their closure | 10 |
| 5. Canonical splitting and mixing operators | 14 |
| 6. A conjecture on the long-time behavior and integrability | 16 |
| Appendix A. Proof of Theorem 4 | 17 |
| References | 22 |

Acknowledgements. The authors would like to thank Michele Dolce and Theo Drivas for fruitful discussions related to this work.

¹DEPARTMENT OF MATHEMATICAL SCIENCES, CHALMERS UNIVERSITY OF TECHNOLOGY AND THE UNIVERSITY OF GOTHENBURG, SE-412 96 GOTHENBURG, SWEDEN

²SCUOLA NORMALE SUPERIORE DI PISA, PISA, ITALY

E-mail addresses: klas.modin@chalmers.se, milo.viviani@sns.it.

Date: May 24, 2024.

2020 *Mathematics Subject Classification.* 35Q31, 53D50, 76M60, 76B47, 53D25.

1. INTRODUCTION

If you stir up an incompressible, low-viscosity fluid confined to a thin (almost 2-D) bounded domain, what you see is spectacular, completely different from the situation in full 3-D. The fluid self-organizes into large, coherently swirling vortex condensates. Some regions swirl counterclockwise (positive vorticity) while others swirl clockwise (negative vorticity), with occasional merger between equal-signed regions, and repulsion between opposite-signed regions. What is the mechanism of vortex condensation and under which conditions does it occur? More mathematically formulated, what is the generic long-time behavior of the 2-D Euler equations?

A milestone was reached in 1949, when Onsager [33] suggested to use statistical mechanics applied to a large but finite number N of point vortices on a flat torus (doubly periodic square). Onsager ingeniously realized that if the energy of a configuration is large enough, the thermodynamical temperature is negative. Point vortices of equal sign will then tend to cluster “so as to use up excess energy at the least possible cost in terms of degrees of freedom” [33, p. 281]. Thus, statistical mechanics predicts vortex condensation. Under the ergodicity assumption, it also predicts the long-time states corresponding to “thermal equilibrium”. Onsager’s ideas have fostered several mathematically rigorous results, for example weak convergence, in both positive and negative temperature regimes, of the canonical Gibbs measure as $N \rightarrow \infty$ [2, 22]. However, there is a problem with the point vortex approach, as Onsager himself pointed out: “When we compare our idealised model with reality, we have to admit one profound difference: the distribution of vorticity which occur in the actual flow of normal liquids are continuous” [33, p. 281]. In particular, solutions to the 2-D Euler equations with continuous vorticity (more precisely L^∞) possess a rich geometric structure: they are described by an infinite-dimensional Lie–Poisson system, which gives rise to infinitely many conservation laws given by Casimir functions (*cf.* Sec. 2 below). These Casimirs are not preserved (not even defined) in the point vortex model. Yet, there is evidence that the Casimirs significantly affect the long-time behavior (*cf.* Abramov and Majda [1]). From this perspective, Onsager’s model is not satisfactory. Furthermore, the ergodicity assumption is not valid (which does not, however, wholly invalidate the theory; see the discussion in Marchioro and Pulvirenti [28, Sec. 7.5]).

Another established technique for 2-D hydrodynamics is non-linear PDE analysis. It has provided a flora of rigorous and deep results, but at the cost of somewhat restricted settings, for example perturbations of steady solutions. We refer to the monograph of Marchioro and Pulvirenti [28] and the lecture notes of Šverák [36] for an overview. The grand vision, of course, is to bridge PDE analysis results with predictions from statistical hydrodynamics. It is a notoriously difficult problem. A flavor of the difficulty is captured in the following “incompatibility” between the two approaches: The statistically predicted vortex condensation implies merging of equally signed vorticity regions. Yet, in the 2-D Euler equations, vorticity is transported by the fluid velocity field, so merging can only occur by trapping increasingly narrow, but deep, vorticity variations in an overwhelmingly complicated stretch-and-fold process. These variations cannot “disappear” in the C^1 -topology required for the strong formulation of the governing PDE. Indeed, the C^1 -norm along regular solutions can, and in numerical simulations typically does, grow extremely fast (e.g., double exponential [24]).

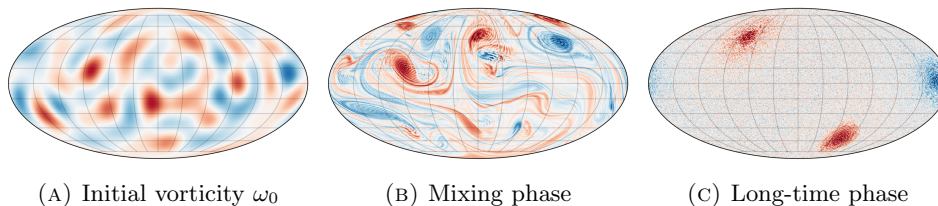


FIGURE 1. A numerical simulation of the vorticity field for Euler’s equations on \mathbb{S}^2 . The results are displayed using the Mollweide area preserving projection. For random smooth initial data (A), the typical dynamical behavior is a mixing phase (B) where vorticity regions of equal sign undergo merging, followed by a long-time phase (C) of 3 or 4 remaining large, weakly interacting vortex condensates whose centers of mass move along nearly quasi periodic trajectories.

A third tool for 2-D hydrodynamics is to carry out numerical experiments (e.g., Fig. 1, where the mixing phase (B) captures a typical stretch-and-fold process). Indeed, since the work of Lorentz [27] in the 1960s, computer simulations have guided numerous analytical results in fluid dynamics; recent examples are found in the references [6, 35, 24, 10, 4, 38]. But how can we know if the numerical results are consistent with the geometric structures principal to the long-time behavior? The key is to ensure that the finite-dimensional dynamical model resulting from the discretization is itself a Lie–Poisson system. Such a model was provided by Zeitlin [40, 41], based on quantization results of Hoppe [16, 17]. It is the only known self-consistent spatial discretization of 2-D Euler, yet surprisingly underexplored.

Our paper draws from the following observation: in addition to numerical advantages, *matrix hydrodynamics* – the isospectral matrix flows enabled via Zeitlin’s model – brings theoretical insights to classical 2-D hydrodynamics, as it provides a link to matrix theory with all its findings. We therefore advocate matrix hydrodynamics as a tool for 2-D turbulence, similar in spirit to the point vortex model of Onsager, but with the benefit that it captures the Lie–Poisson geometry of continuous vorticity fields, including conservation of Casimirs. In addition to the examples in this paper, a motivation and feasibility check for the approach comes from complex geometry. Indeed, in the late 1980s, quantization was promoted to address problems related to Kähler–Einstein metrics and the Calabi conjecture. Tian [37] then gave convergence results, since used regularly in theoretical contexts. Only much later did Donaldson [8] use quantization in a numerical study of Kähler–Einstein metrics. This is the antithesis to the developments in 2-D hydrodynamics, where Zeitlin’s model has been a numerical tool, until recently.

The primary aim of the paper is to give basic convergence results endorsing matrix hydrodynamics as an approach (Theorem 4, Theorem 6, Corollary 14, and Theorem 16), and to showcase the notion in selected examples and relate it to existing theories (Sec. 4-6). The secondary aim, addressed in Sec. 3, is to give a transparent derivation of Zeitlin’s model on the sphere, based on unitary representation theory and focused on geometry rather than algebraic formulae. Before that, we review in Sec. 2 the full geometric structure of the 2-D Euler equations.

2. BACKGROUND: GEOMETRY OF THE 2-D EULER EQUATIONS

Consider a domain filled with an infinite number of fluid particles that push each other in a frictionless, incompressible way. For such systems, Euler [11] showed how Newton's equations give rise to a set of partial differential equations (PDEs) for the velocity field $\mathbf{v}(x, t)$ of the particles' motion,

$$\frac{\partial \mathbf{v}}{\partial t} + \nabla_{\mathbf{v}} \mathbf{v} = -\nabla p, \quad \operatorname{div} \mathbf{v} = 0, \quad (1)$$

where p is the pressure function and $\nabla_{\mathbf{v}}$ is the co-variant derivative. Euler's equations (1) make sense on any Riemannian manifold, but in 2-D the geometric structure is richer than in higher dimensions, and the dynamics is significantly different. Throughout this paper we shall work on the sphere \mathbb{S}^2 , partly because of its relevance in geophysical contexts, but mostly because it later allows a description in terms of unitary representation theory that renders the geometric structures in Zeitlin's model more transparent.

Let $J: T\mathbb{S}^2 \rightarrow T\mathbb{S}^2$ denote the bundle mapping for rotation by $\pi/2$ in positive direction. The curl operator maps the vector field \mathbf{v} on \mathbb{S}^2 to the *vorticity function*

$$\omega = \operatorname{curl} \mathbf{v} \equiv \operatorname{div}(J\mathbf{v}).$$

Since $\operatorname{curl} \circ \nabla \equiv 0$, we obtain from Euler's equations (1) that ω fulfills the transport equation

$$\frac{\partial \omega}{\partial t} + \operatorname{div}(\omega \mathbf{v}) = 0.$$

Further, since the first co-homology of the sphere is trivial, it follows from Hodge theory that the divergence free vector field \mathbf{v} can be written $\mathbf{v} = \nabla^{\perp} \psi \equiv -J\nabla \psi$, where ψ is the *stream function*, unique up to a constant. Euler's equations (1) can now be written entirely in terms of the vorticity and stream functions

$$\frac{\partial \omega}{\partial t} + \operatorname{div}(\omega \nabla^{\perp} \psi) = 0, \quad \Delta \psi = \omega. \quad (2)$$

We now demonstrate how to arrive at these equations from the point-of-view of symplectic geometry and Hamiltonian dynamics.

The sphere is a symplectic manifold for the symplectic form given by the spherical area form μ (in spherical coordinates $(\theta, \phi) \in [0, \pi] \times [0, 2\pi)$ the area form is given by $\mu = \sin \theta \, d\theta \wedge d\phi$). Given a Hamiltonian function f on \mathbb{S}^2 , the corresponding symplectic vector field X_f is defined by

$$\iota_{X_f} \mu = df. \quad (3)$$

If we identify 1-forms with vector fields using the Riemannian structure of \mathbb{S}^2 , equation (3) takes the form

$$JX_f = \nabla f \iff X_f = -J\nabla f.$$

Thus, the fluid velocity field is the symplectic vector field for the Hamiltonian given by the stream function: $\mathbf{v} = X_{\psi}$.

The space $\mathfrak{X}_{\mu}(\mathbb{S}^2)$ of smooth, symplectic vector fields on \mathbb{S}^2 forms an infinite-dimensional Lie algebra (with the vector field bracket $[\cdot, \cdot]_{\mathfrak{X}}$). This algebra is isomorphic to the Poisson algebra of smooth functions modulo constants $C^{\infty}(\mathbb{S}^2)/\mathbb{R}$ via the mapping $\psi \mapsto X_{\psi}$. Indeed, we have that

$$-[X_{\psi}, X_{\xi}]_{\mathfrak{X}} = \{\psi, \xi\} = \nabla^{\perp} \psi \cdot \nabla \xi.$$

Let us now describe the connection between this infinite-dimensional Lie algebra and the vorticity equation (2).

Let \mathfrak{g} be a Lie algebra. Its dual \mathfrak{g}^* is a Poisson manifold via its *Lie–Poisson bracket*. In the infinite-dimensional case of smooth Hamiltonian (or stream) functions, i.e., $\mathfrak{g} = C^\infty(\mathbb{S}^2)/\mathbb{R}$, one usually works with the *smooth dual*, which is constructed so that $C^\infty(\mathbb{S}^2)^* \simeq C^\infty(\mathbb{S}^2)$ via the L^2 -pairing $\langle \omega, \psi \rangle = \int_{\mathbb{S}^2} \omega \psi \mu$. As indicated, we think of vorticity ω as a dual variable to the stream function $\psi \in \mathfrak{g} = C^\infty(\mathbb{S}^2)/\mathbb{R}$. Thus,

$$\omega \in \mathfrak{g}^* = (C^\infty(\mathbb{S}^2)/\mathbb{R})^* \simeq C_0^\infty(\mathbb{S}^2) = \{f \in C^\infty(\mathbb{S}^2) \mid \int_{\mathbb{S}^2} f \mu = 0\}.$$

In other words, the smooth dual of the Lie algebra of Hamiltonian functions (or equivalently symplectic vector fields) is given by smooth functions with vanishing mean.

Now, the Hamiltonian system on the Lie–Poisson space \mathfrak{g}^* for a Hamiltonian function $H: \mathfrak{g}^* \rightarrow \mathbb{R}$ is formally given by

$$\dot{\omega} + \text{ad}_{\frac{\delta H}{\delta \omega}}^* \omega = 0 \tag{4}$$

where $\dot{\omega}$ denotes time differentiation and $\text{ad}_f^*: \mathfrak{g}^* \rightarrow \mathfrak{g}^*$ is defined by $\langle \text{ad}_f^* \omega, \xi \rangle = \langle \omega, \{f, \xi\} \rangle$ for all $\xi \in \mathfrak{g}$. In the case $\mathfrak{g} = C^\infty(\mathbb{S}^2)/\mathbb{R}$, with smooth dual $\mathfrak{g}^* = C_0^\infty(\mathbb{S}^2)$, we obtain from the divergence theorem that

$$\langle \omega, \{f, \xi\} \rangle = \int_{\mathbb{S}^2} \omega \nabla^\perp f \cdot \nabla \xi \mu = \langle -\text{div}(\omega \nabla^\perp f), \xi \rangle = \underbrace{\langle -\{f, \omega\}, \xi \rangle}_{\text{ad}_f^* \omega}.$$

Hence, $\text{ad}_f^* \omega$ is minus the Poisson bracket, which reflects that the L^2 -pairing on the Poisson space $C^\infty(\mathbb{S}^2)$ is bi-invariant.

Equation (2), for the evolution of vorticity, can now be written as a Lie–Poisson system for the quadratic Hamiltonian

$$H(\omega) = \frac{1}{2} \int_{\mathbb{S}^2} |\nabla \psi|^2 \mu = -\frac{1}{2} \int_{\mathbb{S}^2} \omega \underbrace{\Delta^{-1} \omega}_\psi \mu.$$

Its variational derivative is $\frac{\delta H}{\delta \omega} = -\psi$. Consequently, the Lie–Poisson form (4) of equation (2) is

$$\dot{\omega} + \{\psi, \omega\} = 0, \quad \Delta \psi = \omega, \tag{5}$$

where we think of the Laplacian as an isomorphism between \mathfrak{g} and \mathfrak{g}^* , i.e.,

$$\Delta: C^\infty(\mathbb{S}^2)/\mathbb{R} \rightarrow C_0^\infty(\mathbb{S}^2).$$

Equation (5) is the starting point for Zeitlin’s model: the notion is to replace the infinite-dimensional Lie algebra \mathfrak{g} with a finite-dimensional one and then consider the corresponding Lie–Poisson system. We give the details in the next section. Here, we continue with a re-formulation of equation (5) that reveals the connection to the Lie group of \mathfrak{g} .

From (5) it is clear that the vorticity function ω is infinitesimally transported by the time-dependent Hamiltonian vector field $\mathbf{v} = X_\psi$. Consequently, the flow map $\Phi: \mathbb{S}^2 \times \mathbb{R} \rightarrow \mathbb{S}^2$ obtained by integrating the vector field

$$\frac{\partial \Phi(x, t)}{\partial t} = \mathbf{v}(\Phi(x, t), t), \quad \Phi(x, 0) = x,$$

is a curve $t \mapsto \Phi(\cdot, t)$ in the Lie group G corresponding to the Lie algebra \mathfrak{g} . Since the integration of a vector field yields a symplectic map if and only if the vector field is symplectic, it follows that the Lie group consists of symplectic diffeomorphisms of \mathbb{S}^2 , denoted $\text{Diff}_\mu(\mathbb{S}^2)$. Since ω is transported, we have that $\omega(x, t) = \omega(\Phi^{-1}(x, t), 0)$, or in more compact notation $\omega_t = \omega_0 \circ \Phi_t^{-1}$. The direct implication is that ω remains on the same *co-adjoint orbit* as ω_0 (the orbits for the action of $\text{Diff}_\mu(\mathbb{S}^2)$ on $C_0^\infty(\mathbb{S}^2)$). Therefore, since the map Φ_t has unitary Jacobian determinant, any functional of the form

$$C_f(\omega) = \frac{1}{2\pi} \int_{\mathbb{S}^2} f(\omega(x, t)) \mu(x), \quad f: \mathbb{R} \rightarrow \mathbb{R},$$

is conserved: these are the *Casimir functions*.

In addition to Casimirs, the transport property implies weak (distributional), finite-dimensional co-adjoint orbits given by n interacting point vortices

$$\omega = \sum_{k=1}^n \Gamma_k \delta_{x_k}.$$

These were found by Helmholtz [14], and analyzed by Kirchhoff [23] and Kelvin [20]. Much later, Onsager [33] used them in his theory of statistical hydrodynamics. The existence of weak solutions shows that the restriction to the smooth dual is not always legitimate.

Instead of ω_t as dynamic variable, we can use the transport map $\Phi_t \in \text{Diff}_\mu(\mathbb{S}^2)$ via the equation

$$\dot{\Phi}_t = X_\psi \circ \Phi_t, \quad \Delta\psi = \omega_0 \circ \Phi_t^{-1}. \quad (6)$$

This is the *transport map formulation* of equation (5). Notice that ω is not required to be differentiable here, which is the key to Yudovich's [39] global well-posedness results in L^∞ .

What happens with the Hamiltonian structure when we switch to the transport formulation in (6)? Interestingly, the group $\text{Diff}_\mu(\mathbb{S}^2)$ inherits the symplectic structure of \mathbb{S}^2 . Indeed, as an infinite-dimensional Lie group, the tangent bundle TG is trivializable as $G \times \mathfrak{g}$ via right translation. The symplectic structure is then

$$T_\Phi G \times T_\Phi G \simeq \mathfrak{g} \times \mathfrak{g} \ni (\psi, \xi) \mapsto \int_{\mathbb{S}^2} \{\psi, \xi\} \mu.$$

With this symplectic structure, equation (6) is Hamilton's equation on $G = \text{Diff}_\mu(\mathbb{S}^2)$ for the Hamiltonian $\bar{H}(\Phi) = H(\omega_0 \circ \Phi^{-1})$.

We have thus summarized the complete geometric description of the 2-D Euler equations on \mathbb{S}^2 . Indeed, the structures presented – the Hamiltonian formulation, the co-adjoint orbits, the conservation of Casimirs, and the transport formulation – are all important in the various mathematical theories for long-time behavior (*cf.* surveys by Drivas and Elgindi [9] and Khesin, Misiołek, and Shnirelman [21]).

3. QUANTIZATION AND THE EULER–ZEITLIN EQUATION

Here are the steps leading to Zeitlin's model on the sphere:

- (1) The first ingredient is an explicit, finite-dimensional quantization of the Poisson algebra $(C^\infty(\mathbb{S}^2), \{\cdot, \cdot\})$. That is, a sequence of linear maps

$$T_N: C^\infty(\mathbb{S}^2) \rightarrow \mathfrak{u}(N)$$

such that, in some sense, the Poisson bracket is approximated by the matrix commutator:

$$T_N(\{\psi, \omega\}) \rightarrow \frac{1}{\hbar}[T_N\psi, T_N\omega] \quad \text{as } N \rightarrow \infty,$$

where $\hbar \sim 1/N$. Notice that the convergence cannot be uniform in ψ and ω , since $C^\infty(\mathbb{S}^2)$ is infinite-dimensional.

- (2) The projection maps T_N should take the unit function $x \mapsto 1$ to the imaginary identity matrix $iI \in \mathfrak{u}(N)$. In particular, T_N descends to a map between the quotient Lie algebras $C^\infty(\mathbb{S}^2)/\mathbb{R}$ and $\mathfrak{pu}(N) \equiv \mathfrak{u}(N)/i\mathbb{R}I$.¹
- (3) The dual $\mathfrak{pu}(N)^*$ is naturally identified with $\mathfrak{su}(N)$ via the pairing $\langle W, P \rangle = -\text{tr}(WP)$ for $P \in \mathfrak{pu}(N)$ and $W \in \mathfrak{su}(N)$. The corresponding ad^* -operator on $\mathfrak{su}(N)$ is

$$\text{ad}_P^* W = -\frac{1}{\hbar}[P, W].$$

- (4) The last ingredient is a “quantized” Laplace operator $\Delta_N: \mathfrak{u}(N) \rightarrow \mathfrak{su}(N)$. It should have the kernel $i\mathbb{R}I$ and descend to a bijective map $\mathfrak{pu}(N) \rightarrow \mathfrak{su}(N)$. Zeitlin’s model is then the Lie–Poisson system on $\mathfrak{g}^* = \mathfrak{pu}(N)^* \simeq \mathfrak{su}(N)$, given by the isospectral flow

$$\dot{W} + \frac{1}{\hbar}[P, W] = 0, \quad \Delta_N P = W. \quad (7)$$

3.1. Quantization via representation. To build the quantization maps T_N , it is natural to begin from the sphere’s symmetry: the Lie group $\text{SO}(3)$. The connection to the space of functions $C^\infty(\mathbb{S}^2)$ is established via its Lie algebra $\mathfrak{so}(3)$ as follows. Let $x_1, x_2, x_3 \in C^\infty(\mathbb{S}^2)$ be a choice of Euclidean coordinate functions for the embedded sphere $\mathbb{S}^2 \subset \mathbb{R}^3$. These functions generate $\mathfrak{so}(3)$ as a Lie sub-algebra of the Poisson algebra $\mathfrak{g} = (C^\infty(\mathbb{S}^2), \{\cdot, \cdot\})$. But we should think of it differently. Namely, the basis elements $\mathbf{e}_1, \mathbf{e}_2, \mathbf{e}_3 \in \mathbb{R}^3 \simeq \mathfrak{so}(3)$ are associated with first order differential operators \mathcal{X}_i on $C^\infty(\mathbb{S}^2)$ given by

$$\mathcal{X}_\alpha \omega = \{x_\alpha, \omega\}.$$

Then $\mathcal{X}_1, \mathcal{X}_2, \mathcal{X}_3$ provides a unitary representation of $\mathfrak{so}(3)$ on $C^\infty(\mathbb{S}^2)$ compatible with the Poisson algebra structure. Indeed, the Jacobi identity yields $\mathcal{X}_\alpha \mathcal{X}_\beta - \mathcal{X}_\beta \mathcal{X}_\alpha = \{\{x_\alpha, x_\beta\}, \cdot\}$ and each \mathcal{X}_α is skew self-adjoint with respect to the L^2 inner product. We now apply the powerful machinery of Schur, Cartan, Weyl, and others (cf. [25]) for representations of compact groups and the connection to harmonic analysis. First, the generators $\mathcal{X}_1, \mathcal{X}_2, \mathcal{X}_3$ can be viewed as the first order elements of the *universal enveloping algebra* $U(\mathfrak{so}(3))$. Higher order elements correspond to higher order differential operators. In particular, the Killing form on $\mathfrak{so}(3)$ corresponds to the second order *Casimir element* $\mathcal{C} = -\sum_\alpha \mathcal{X}_\alpha^2$, which in this case is the Laplacian Δ on \mathbb{S}^2 . The Casimir element commutes with each \mathcal{X}_α . In particular, if $V \subset C^\infty(\mathbb{S}^2)$ is an eigenspace of $\mathcal{C} = \Delta$ with eigenvalue λ , then $\mathcal{X}_1, \mathcal{X}_2, \mathcal{X}_3$ provide a sub-representation of $\mathfrak{so}(3)$ on V . Indeed, $\mathcal{C}[\mathcal{X}_\alpha, \mathcal{X}_\beta]V = [\mathcal{X}_\alpha, \mathcal{X}_\beta]\mathcal{C}V = \lambda[\mathcal{X}_\alpha, \mathcal{X}_\beta]V$, so $[\mathcal{X}_\alpha, \mathcal{X}_\beta]V$ must belong to the eigenspace of λ , i.e., $[\mathcal{X}_\alpha, \mathcal{X}_\beta]V \subset V$. One can further prove that this representation is irreducible. In fact, the eigenspaces V_ℓ for $\lambda_\ell = -\ell(1 + \ell)$, $\ell = 0, 1, \dots$ correspond to all the irreducible infinitesimal representations of $\text{SO}(3)$ (i.e., the odd-dimensional representations of

¹We refrain from identifying the Lie algebra $\mathfrak{pu}(N)$ with $\mathfrak{su}(N)$, since its Lie group $\text{PU}(N)$ is different from $\text{SU}(N)$.

$\mathfrak{so}(3)$). Furthermore, V_ℓ has dimension $2\ell + 1$ and comes with a canonical basis $Y_{\ell m}$ (the spherical harmonics) corresponding to the *weights* $m = -\ell, \dots, \ell$ of the representation.

From the point of view just presented, the aim of quantization is to construct a representation of $\mathfrak{so}(3)$ on the Lie algebra $\mathfrak{u}(N)$, which should be ‘as large as possible’: since $\mathfrak{u}(N) \simeq V_0 \oplus \dots \oplus V_{N-1}$ as vector spaces one can hope to capture all the irreducible representations V_ℓ for $\ell = 0, \dots, N-1$. By identifying the canonical basis $Y_{\ell m}$ in $\mathfrak{u}(N)$, we then obtain the projection $T_N: \mathfrak{g} \rightarrow \mathfrak{u}(N)$. Following Hoppe and Yau [18], but focusing on geometry rather than formulae, we now give a recipe for such a construction.

For N even or odd, corresponding to $\ell' = (N-1)/2$, begin with an irreducible, unitary representation $\pi: \mathfrak{so}(3) \rightarrow \mathfrak{u}(N)$. Let $S_\alpha = \pi(\mathbf{e}_\alpha)$, chosen so that S_3 is diagonal with sorted, equidistant eigenvalues $-i\ell', \dots, i\ell'$ corresponding to the weights of the representation. Since the representation is unitary, S_1, S_2, S_3 share the same spectrum.

The Casimir element restricted to the representation is just multiplication by $-\ell'(1+\ell')$ and is therefore given by the diagonal matrix $C = -\sum_\alpha S_\alpha^2 = -\ell'(1+\ell')I$. We now introduce a scaled representation $X_\alpha = \hbar S_\alpha$ in such a way that the matrix X_α correspond to the function x_α on \mathbb{S}^2 . Thus, to achieve $(\sum_\alpha X_\alpha^2)^{1/2} = iI$, corresponding to $(\sum_\alpha x_\alpha^2)^{1/2} = 1$, we take $\hbar = 1/\sqrt{\ell'(1+\ell')} = 2/\sqrt{N^2-1} =: \hbar_N$.

From the representation on $\mathbb{C}^N \simeq V_{\ell'}$ we obtain another on $\mathfrak{u}(N)$: for $W \in \mathfrak{u}(N)$, the infinitesimal action of \mathbf{e}_α on W is

$$\mathbf{e}_\alpha \cdot W = [S_\alpha, W] = \frac{1}{\hbar} [X_\alpha, W].$$

The Casimir element for this representation is the *Hoppe–Yau Laplacian*

$$\Delta_N: \mathfrak{u}(N) \rightarrow \mathfrak{u}(N)$$

given by

$$\Delta_N = \sum_{\alpha=1}^3 [S_\alpha, [S_\alpha, \cdot]] = \frac{1}{\hbar^2} \sum_{\alpha=1}^3 [X_\alpha, [X_\alpha, \cdot]].$$

Being the Casimir element, any eigenvalue is of the form $\lambda = -\ell(1+\ell)$ for some $\ell \in \mathbb{N}/2$ and the corresponding eigenspace V_ℓ has dimension $2\ell+1$. From the Peter–Weyl theorem, the representation on $\mathfrak{u}(N)$ decomposes into irreducible, orthogonal components $\mathfrak{u}(N) \simeq V_{\ell_0} \oplus \dots \oplus V_{\ell_{n-1}}$. But which ℓ_k are included?

Since $\Delta_N iI = 0$ and $\Delta_N X_\alpha = 2X_\alpha$, we have $\ell_0 = 0$ and $\ell_1 = 1$. More generally and as desired, $\ell_k = k$ and $n = N$:

Lemma 1. $\mathfrak{u}(N) \simeq V_0 \oplus \dots \oplus V_{N-1}$ where V_ℓ decomposes orthogonally as

$$V_\ell = \bigoplus_{m=0}^{\ell} V_{\ell m}, \quad \text{with} \quad \dim V_{\ell m} = \begin{cases} 1 & \text{if } m = 0 \\ 2 & \text{if } m \neq 0. \end{cases}$$

The components $V_{\ell m}$, corresponding to the weights $\pm 2m$, are mapped to the $\pm m$ th diagonals of the matrix in $\mathfrak{u}(N)$.

Proof. Consider the space $\text{poly}_N = \{p \in \mathbb{C}[x] \mid \deg p = N\}$ of polynomials. A bijection between diagonal matrices $D(N)$ and poly_N is given by $p \mapsto p(X_3)$. This is an algebra isomorphism, since $(pq)(X_3) = p(X_3)q(X_3)$. Let p_ℓ denote the Legendre

polynomials and consider the corresponding matrices $P_\ell = p_\ell(X_3)$. One can readily check that $\Delta_N P_\ell$ is diagonal and corresponds to the polynomial

$$\frac{d}{dx}(1-x^2)\frac{d}{dx}p_\ell(x).$$

From Sturm–Liouville theory it then follows that $\Delta_N P_\ell = -\ell(\ell+1)P_\ell$. Thus, we must have that the representation on $\mathfrak{u}(N)$ includes V_ℓ for $\ell = 0, \dots, N-1$. By a dimension count, it then follows that $\mathfrak{u}(N) \simeq V_0 \oplus \dots \oplus V_{N-1}$. To see that each V_ℓ decomposes as stated, one can introduce the “shift operators” X and Y obtained as part of the standard basis H, X, Y in the complexification $\mathfrak{sl}(2, \mathbb{C}) \simeq \mathfrak{su}(2)_\mathbb{C}$. Since X and Y has elements only on the first upper and lower diagonal respectively, it follows from representation theory for $\mathfrak{sl}(2, \mathbb{C})$ that $P_\ell \in V_\ell$ gives rise to 2ℓ new basis vectors $P_{\ell m} \in V_\ell \otimes \mathbb{C}$ for $m = -\ell, \dots, \ell$ with $P_{\ell 0} = P_\ell$, each of which is supported on the m :th diagonal. Another dimension count then concludes that this basis spans $V_\ell \otimes \mathbb{C}$, so the corresponding real basis

$$\frac{1}{2} \left(P_{\ell m} - P_{\ell(-m)}^\dagger \right) \quad \text{and} \quad \frac{i}{2} \left(P_{\ell m} + P_{\ell(-m)}^\dagger \right) \quad \text{spans } V_\ell.$$

□

Remark 1. For N even, i.e., the $\ell' = (N-1)/2$ “half-integer spin” representation on \mathbb{C}^N , we still obtain only “integer spin” representations on $\mathfrak{u}(N)$. This is desirable, since the eigenspaces of the Laplacian on \mathbb{S}^2 correspond exactly to the integer spin (odd-dimensional) representations of $\mathfrak{so}(3)$.

The decomposition in Lemma 1 enables explicit construction of the projection map $T_N: \mathfrak{g} \rightarrow \mathfrak{u}(N)$. Indeed, the $\pm m$ th diagonals of $W \in \mathfrak{u}(N)$ are spanned by $V_{:m} := V_{mm} \oplus \dots \oplus V_{(N-1)m} \simeq \mathbb{C}^{N-m}$. In turn, $V_{:m}$ corresponds to the span of the spherical harmonic functions $Y_{mm}, \dots, Y_{(N-1)m}$. Since $\Delta_N V_{:m} \subseteq V_{:m}$, we obtain the $\pm m$ diagonals by identifying the eigenvector of $\Delta_N|_{V_{:m}}$ with eigenvalue $-(m+k)(1+m+k)$ with the spherical harmonic function $Y_{(m+k)m}$. Specifically, $\Delta_N|_{V_{:m}}: \mathbb{C}^{N-m} \rightarrow \mathbb{C}^{N-m}$, as an operator acting on the upper m th diagonal of W , is a tridiagonal, symmetric matrix. The spectral decomposition of $\Delta_N|_{V_{:m}}$ can hence be computed by efficient numerical methods of complexity $\mathcal{O}(N)$. This way, a function $\omega \in \mathfrak{g}$ is projected to the matrix $W = T_N \omega$ from its spherical harmonics coefficients $(\omega_{\ell m})_{\ell \leq N-1}$ in only $\mathcal{O}(N^2)$ numerical operations; see Cifani *et al.* [5] for details. Notice that the L^2 dual $T_N^*: \mathfrak{u}(N) \rightarrow \mathfrak{g}$ is a right inverse of T_N .

We have thus arrived at the following:

Theorem 2 ([18]). *The operators Δ_N and T_N fulfill*

- $T_N \Delta \omega = \Delta_N T_N \omega$;
- $T_N 1 = iI$;
- $T_N \{x_\alpha, \omega\} = \frac{1}{\hbar} [X_\alpha, T_N \omega]$.

This result achieves the steps 2–4 listed above. Moreover, (i) the approximation Δ_N to the Laplacian on \mathbb{S}^2 is exact on the subspace spanned by spherical harmonics up to order $\ell = N-1$, and (ii) the $\text{SO}(3)$ -symmetry of \mathbb{S}^2 is preserved, since $\mathfrak{so}(3)$ is represented analogously on $\mathfrak{u}(N)$ and $C^\infty(\mathbb{S}^2)$.

Remark 2. Zeitlin’s original model on the flat torus does *not* correspond to a representation of the symmetry group, which implies more of Gibb’s phenomenon than in the sphere model.

The remaining step (1) above, relating the Poisson bracket $\{\cdot, \cdot\}$ to the scaled commutator $\frac{1}{\hbar}[\cdot, \cdot]$, is at the heart of quantization theory. The following is a specialization to our setting of a result by Charles and Polterovich [3].

Theorem 3 ([3]). *There exists $\alpha > 0$ so for all $\omega \in C^2(\mathbb{S}^2)$*

$$\|\omega\|_{L^\infty} - \alpha\hbar\|\omega\|_{C^2} \leq \|T_N\omega\|_\infty \leq \|\omega\|_{L^\infty},$$

where $\|W\|_\infty = \sup_{\mathbf{v}} \frac{|W_{\mathbf{v}}|}{|\mathbf{v}|}$. Further, there exists $\beta > 0$ so for all $\omega, \psi \in C^3(\mathbb{S}^2)$

$$\left\| \frac{1}{\hbar}[T_N\omega, T_N\psi] - T_N\{\omega, \psi\} \right\|_\infty \leq \beta\hbar \sum_{k=1}^3 \|\omega\|_{C^k} \|\psi\|_{C^{4-k}}.$$

Remark 3. Since $C^2(\mathbb{S}^2)$ is dense in $L^\infty(\mathbb{S}^2)$, it follows from the first inequality in Theorem 3 that T_N can be extended to a bounded operator $L^\infty(\mathbb{S}^2) \rightarrow \mathfrak{su}(N)$.

Via a bracket convergence result in the L^2 norm (see Lemma 13 of the appendix), instead of the spectral norm as in Theorem 3, we obtain convergence of solutions.

Theorem 4. *Let $\omega(t)$ be a solution of (5), and $W(t)$ the solution of (7) with $W(0) = T_N\omega(0)$. Then, for t fixed, $\|T_N^*W(t) - \omega(t)\|_{L^2} \rightarrow 0$ as $N \rightarrow \infty$.*

Proof. See appendix. □

Remark 4. The result² in Theorem 4 is analogous to the L^2 convergence result of Gallagher [13] for Zeitlin’s original model on the flat torus \mathbb{T}^2 . But there are fundamental differences in the techniques: Gallagher’s result rely on the algebraic multiplication properties of the Fourier basis in \mathbb{T}^2 , which are not available on \mathbb{S}^2 .

4. COADJOINT ORBITS AND THEIR CLOSURE

For initial vorticity ω_0 , consider the orbit $\{S_t(\omega_0) \mid t \geq 0\}$, where S_t is the flow map for the vorticity equation (5). Šverák [36] conjectured that orbits for generic $\omega_0 \in L^\infty(\mathbb{S}^2)$ are not L^2 precompact, which can be interpreted as a mathematical formulation of the “forward enstrophy cascade” in 2-D turbulence (cf. Kraichnan [26]). Of course, the orbits in Zeitlin’s model are always precompact, since they evolve on a finite dimensional sphere. Nevertheless, simulations with increasing N support Šverák’s conjecture.

In Arnold’s geometric viewpoint, it follows from equation (6) that smooth solutions $\omega(t) \in C^\infty(\mathbb{S}^2)$ remain on the *coadjoint orbit* $\mathcal{O}(\omega_0) = \{\omega_0 \circ \Phi \mid \Phi \in \text{Diff}_\mu(\mathbb{S}^2)\}$. A first step in understanding $\{S_t(\omega_0) \mid t \geq 0\}$ is thus to characterize $\mathcal{O}(\omega_0)$, a problem solved by Izosimov, Khesin, and Mousavi [19] via the Reeb graph of ω_0 equipped with a measure reflecting the “density” of the level sets (see Fig. 2a).

Theorem 5 ([19]). *Let $\omega, \psi \in C^\infty(\mathbb{S}^2)$ be simple Morse functions (distinct critical values). Then $\psi \in \mathcal{O}(\omega)$ if and only if ω and ψ have the same measured Reeb graph.*

However, while solutions with smooth initial data remain smooth, the C^k -norms for $k \geq 1$ typically grow fast as the vorticity level-curves quickly become extremely entangled. This mechanism results in a Reeb graph that is well-defined but futile to track at moderate scales. It is therefore natural to study the closure of coadjoint orbits in a weaker topology, for instance L^∞ as Yudovich’s existence theory suggests. In doing so, the measured Reeb graph is not stable in L^∞ since it is based on critical

²See also Theorem 16 of the appendix for a more detailed statement.

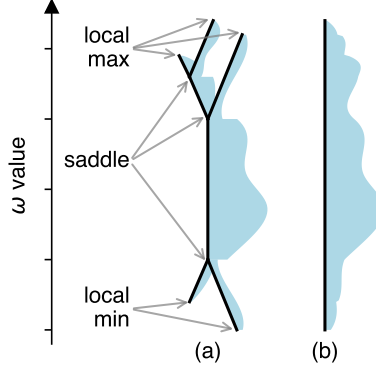


FIGURE 2. **(a)** Measured Reeb graph for a function ω on \mathbb{S}^2 with three local maxima and two local minima. Another function ψ has the same measured Reeb graph if and only if there exists $\Phi \in \text{Diff}_\mu(\mathbb{S}^2)$ such that $\psi = \omega \circ \Phi$ (cf. Theorem 5). **(b)** Level-set measure λ_ω . It is a flattening, via horizontal projection, of the Reeb graph. The measure $\lambda_\omega(I)$ of an interval I is the area of the set $\{x \in \mathbb{S}^2 \mid \omega(x) \in I\}$.

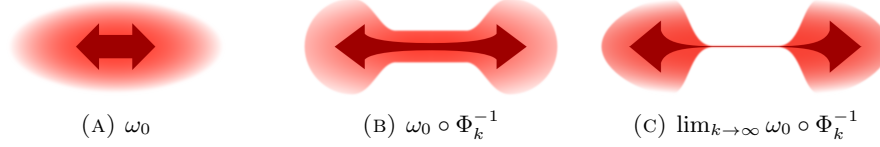


FIGURE 3. Given a vortex configuration ω_0 with one blob, it is possible to find a sequence Φ_k of area-preserving diffeomorphisms which transports it $\omega_0 \circ \Phi_k^{-1}$ such that in the limit $k \rightarrow \infty$ it is L^∞ -indistinguishable from a configuration with two blobs. Thus, the Reeb graph in Theorem 5 is not stable under the L^∞ closure of $\mathcal{O}(\omega_0)$.

values and Morse functions that require C^2 topology (see Fig. 3). Instead, what persists is the *level-set measure* λ_ω , obtained by “flattening” the Reeb graph as follows. The mapping $C^\infty(\mathbb{R}) \ni f \mapsto C_f(\omega)$ is a distribution with compact support, and λ_ω is the corresponding positive Radon measure on \mathbb{R} (see Fig. 2b). The L^∞ closure of a coadjoint orbit then fulfills $\overline{\mathcal{O}(\omega_0)} \subseteq \{\omega \in L^\infty(\mathbb{S}^2) \mid \lambda_\omega = \lambda_{\omega_0}\}$.

But the L^∞ topology is still too strong: it does not permit *vortex mixing*. If $\int_{\mathbb{S}^2} \omega_0 = 0$, one can imagine a sequence Φ_k of increasingly entangling diffeomorphisms for which $\lim_{k \rightarrow \infty} \int_\Omega \omega_0 \circ \Phi_k = 0$ over any open subset $\Omega \subset \mathbb{S}^2$. Yet, however complicated the sequence is, we always have $\|\omega_0 \circ \Phi_k\|_{L^\infty} = \|\omega_0\|_{L^\infty}$. Shnirelman [34] suggested instead the L^∞ weak-* topology, for which $\omega_0 \circ \Phi_k \xrightarrow{*} 0$ is possible. Furthermore, for a generic $\omega_0 \in L^\infty(\mathbb{S}^2)$, the weak-* closure $\overline{\mathcal{O}(\omega_0)}^*$ is convex and can be explicitly characterized [36, 7]. Importantly, the Casimirs C_f are not weak-* continuous (except for $f(z) = z$), so elements in $\overline{\mathcal{O}(\omega_0)}^*$ can have different level-set measures, which signifies vortex mixing.

Matrix hydrodynamics offers a concrete way to address the weak-* topology in 2-D turbulence, as now explained.

The matrix version of the level-set measure λ_ω is the *empirical spectral measure* from random matrix theory. Indeed, $W = T_N(\omega)$ gives rise to the atomic measure $\lambda_W^N = \frac{1}{N} \sum_{k=1}^N \delta_{\lambda_k}$ on \mathbb{R} , where $i\lambda_1, \dots, i\lambda_N$ are the eigenvalues of W .

Theorem 6. *Let $\omega \in C^2(\mathbb{S}^2)$. Then $\lambda_{T_N(\omega)}^N \rightharpoonup \lambda_\omega$ as $N \rightarrow \infty$.*

Proof. Let $I = [\inf \omega, \sup \omega]$ and $f \in C^\infty(I)$. We need to prove that $C_f^N(T_N(\omega)) \rightarrow C_f(\omega)$, which is equivalent to weak convergence of the measure.

We can restrict f to be polynomials, which are dense in $C^\infty(I)$. Since $C_f(\omega) = \sum_m f_m C_{z^m}(\omega)$ and similarly for C_f^N , it is enough to prove that $C_{z^m}^N(T_N\omega) \rightarrow C_{z^m}(\omega)$ for $m = 0, 1, \dots$. Set $W_N = T_N\omega$. Then

$$\begin{aligned} C_{z^m}(W_N) &= \frac{(-i)^m}{N} \operatorname{tr}(W_N^m) = \frac{(-i)^m}{N} \operatorname{tr}(W_N W_N^{m-1}) = \\ &= \frac{(-i)^m}{N} \operatorname{tr}(W_N (W_N^{m-1} - T_N(\omega^{m-1}) + T_N(\omega^{m-1}))) = \\ &= \frac{(-i)^{m-1}}{N} \operatorname{tr}(W_N T_N(\omega^{m-1})) + \operatorname{tr}(W_N (W_N^{m-1} - T_N(\omega^{m-1}))). \end{aligned}$$

Since the scaled Frobenius inner product $-\frac{1}{N} \operatorname{tr}(AB)$ on $\mathfrak{u}(N)$ corresponds to the L^2 inner product, i.e., $\langle T_N^* A, T_N^* B \rangle_{L^2} = -\frac{2\pi}{N} \operatorname{tr}(AB)$, we have

$$\lim_{N \rightarrow \infty} \frac{(-i)^m}{N} \operatorname{tr}(W_N, T_N(\omega^{m-1})) = \frac{1}{2\pi} \langle \omega, \omega^{m-1} \rangle_{L^2} = C_{z^m}(\omega).$$

We also have

$$\begin{aligned} \left| \frac{(-i)^m}{N} \operatorname{tr}(W_N (W_N^{m-1} - T_N(\omega^{m-1}))) \right| &\leq \\ &= \underbrace{\left(\frac{1}{N} \sum_{k=1}^N |\lambda_k| \right)}_{\|W_N\|_1} \|W_N^{m-1} - T_N(\omega^{m-1})\|_\infty \rightarrow 0, \end{aligned}$$

which follows from Lemma 7 below □

Lemma 7. *Let $\omega \in C^2(\mathbb{S}^2)$. Then $\|T_N(\omega)^m - T_N(\omega^m)\|_\infty \rightarrow 0$ as $N \rightarrow \infty$.*

Proof. The result is true for $m = 1$. Assume it for $m - 1$. With $W_N = T_N(\omega)$ we have

$$\begin{aligned} \|W_N^m - T_N(\omega^m)\|_\infty &= \\ \|W_N W_N^{m-1} - T_N(\omega^m) + W_N T_N(\omega^{m-1}) - W_N T_N(\omega^{m-1})\|_\infty &\leq \\ \|W_N (W_N^{m-1} - T_N(\omega^{m-1}))\|_\infty + \\ \|T_N(\omega \omega^{m-1}) - W_N T_N(\omega^{m-1})\|_\infty &\leq \\ \|W_N\|_1 \|W_N^{m-1} - T_N(\omega^{m-1})\|_\infty + \\ \|T_N(\omega \omega^{m-1}) - W_N T_N(\omega^{m-1})\|_\infty. \end{aligned}$$

That the first term vanishes as $N \rightarrow \infty$ follows from the assumption. That the second term vanishes follows from product estimates in quantization theory [3, prop. 3.12]. □

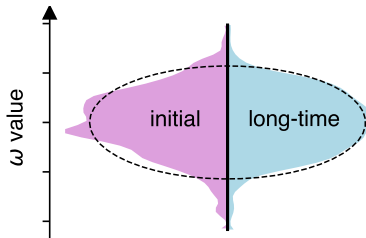


FIGURE 4. The simulation $W(t) \in \mathfrak{su}(512)$ in Fig. 1 is projected to $\tilde{W}(t) \in \mathfrak{su}(480)$. The empirical spectral measure $\lambda_{\tilde{W}(t)}^{480}$ is then displayed at the initial (left) and final (right) time. We observe some tendency towards the Wigner semicircle distribution (dashed curve), except the rims survive due to vortex blobs (compare Fig. 1c).

The level-set measure λ_ω is invariant under the Euler flow (5). Likewise, λ_W^N is invariant under the Euler–Zeitlin flow (7). In particular, for any $f \in C^\infty(\mathbb{R})$ the function $C_f^N(W) = \int_{\mathbb{R}} f d\lambda_W^N$ is a Casimir for $\mathfrak{su}(N)$. A direct corollary of Theorem 6 is that $C_f^N(T_N(\omega)) \rightarrow C_f(\omega)$ as $N \rightarrow \infty$. In this sense, the Euler–Zeitlin equation nearly conserves all Casimirs of the vorticity equation.

The coadjoint action of $F \in \text{SU}(N)$ on $W \in \mathfrak{su}(N)$ is FWF^\dagger . From the spectral theorem it then follows that the coadjoint orbit $\mathcal{O}^N(W) = \{FWF^\dagger \mid F \in \text{SU}(N)\}$ consists of all elements in $\mathfrak{su}(N)$ with the same spectrum as W , or, equivalently, the same empirical measure λ_W^N . It is instructive to compare with the $\text{Diff}_\mu(\mathbb{S}^2)$ coadjoint orbits: in spirit, $\mathcal{O}^N(W)$ corresponds to $\{\omega \in L^\infty(\mathbb{S}^2) \mid \lambda_\omega = \lambda_{\omega_0}\}$, situated between the smooth orbit $\mathcal{O}(\omega)$ (characterized by its measured Reeb graph) and Shnirelman’s weak closure $\overline{\mathcal{O}(\omega_0)}^*$ (characterized by “convex” vortex mixing, cf. [7]).

For a fixed N , matrix hydrodynamics thereby behaves as the Euler equations in the strong L^∞ topology: Casimirs are exactly conserved. But we can also regard all N simultaneously, which gives a hierarchy of increasingly refined topologies.

Definition 1. Let $\mathcal{B}_r = \{\omega \in L^\infty(\mathbb{S}^2) \mid \|\omega\|_{L^\infty} \leq r\}$. The *matrix topology* on \mathcal{B}_r is the Fréchet topology defined by the semi-norms

$$|\omega|_N := \|T_N \omega\|_\infty.$$

The semi-norm $|\cdot|_N$ can “see” structures down to the length scale \hbar_N . Furthermore, each length scale \hbar_N gives an associated truncated level-set measure $\lambda_{T_N(\omega)}^N$. To study how it varies, for fixed N as $t \rightarrow \infty$, gives information about vortex mixing relative to the scale \hbar_N and a connection to random matrix theory (see Fig 4).

The following result connects matrix hydrodynamics to Shnirelman’s notion of weak-* vortex mixing.

Lemma 8. *The matrix topology is equivalent to the weak-* topology on \mathcal{B}_r .*

Proof. The set $V = \{f \mid \exists N : f \in T_N^* \mathfrak{su}(N)\}$ is dense in $L^1(\mathbb{S}^2)$. For $\omega \in L^\infty(\mathbb{S}^2)$ and a test function $f = T_N^* W \in V$ we have

$$|\langle \omega, f \rangle| = |\langle \omega, T_N^* W \rangle| = \frac{2\pi}{N} |\text{tr}(W T_N \omega)| \leq \frac{2\pi}{N} |\omega|_N \|W\|_1.$$

Thus, if, for any N , $|\omega_k|_N \rightarrow 0$ as $k \rightarrow \infty$, then $\langle \omega_k, f \rangle \rightarrow 0$ for all $f \in V$, which implies weak-* convergence since the sequence ω_k in \mathcal{B}_r is bounded in L^∞ -norm. On the other hand, assuming that $\omega_k \rightharpoonup^* 0$, it follows that each spherical harmonic coefficient $(\omega_k)_{\ell m} \rightarrow 0$ as $k \rightarrow \infty$. Thus, since $T_N \omega$ is expanded in a finite basis with the spherical harmonic coefficients, it follows that $\|T_N \omega_k\|_\infty \rightarrow 0$ as $k \rightarrow \infty$. \square

Thus, a plausible relaxation of Euler's equations (5) to the weak-* topology is to consider the Euler–Zeitlin equation (7) *simultaneously for all* $N \geq N_0$. Via the mappings $T_{N-1} \circ T_N^* : \mathbf{u}(N) \rightarrow \mathbf{u}(N-1)$ one can consider an inverse limit $\mathbf{g} = \varprojlim \mathbf{u}(N)$. But this construction is too rigid, since \mathbf{g} is not invariant under the simultaneous Euler–Zeitlin flow. An open problem is to relax the inverse limit, for example based on the equivalence $\{W'_i\}_{i=N_0}^\infty \sim \{W_i\}_{i=N_0}^\infty$ if $\lim_{i \rightarrow \infty} \|W'_i - W_i\|_\infty = 0$, and then prove that the simultaneous Euler–Zeitlin flow is well-defined on equivalence classes. For such a construction, global existence is built-in (albeit not uniqueness).

5. CANONICAL SPLITTING AND MIXING OPERATORS

We now showcase a technique in 2-D turbulence enabled via matrix hydrodynamics: *canonical scale separation* [32].

Stationary solutions of the Euler–Zeitlin equations (7) are characterized by the relation $[P, W] = 0$. The *stabilizer* of P is the subspace $\text{stab}_P = \{W \in \mathfrak{su}(N) \mid [P, W] = 0\}$. For a state W and $P = \Delta_N^{-1} W$, the distance of W to stab_P thus measures how far from stationary the state is.

Let Π_P denote the L^2 projection onto stab_P . It induces a canonical splitting $W = W_s + W_r$ where $W_s = \Pi_P W$. Explicitly, if $E \in U(N)$ is an eigen basis for P , then $\Pi_P(W) = E^* \text{diag}(EWE^*)E$, where diag is the orthogonal projection onto the space of diagonal matrices. From this formula, we can express the Euler–Zeitlin equations in the variables W_s and W_r :

$$\begin{aligned} \dot{W}_s &= [B, W_s] - \Pi_P[B, W_r] \\ \dot{W}_r &= [P, W_r] - [B, W_s] + \Pi_P[B, W_r], \end{aligned} \tag{8}$$

where B is the unique element in the L^2 complement stab_P^\perp such that $[B, P] = \Pi_P^\perp \Delta^{-1}[P, W]$. By construction, the decomposition is orthogonal in L^2 . Curiously, it also fulfills a “reversed” orthogonally condition with respect to the energy norm $\|W\|_E^2 := \langle W, \Delta_N^{-1} W \rangle_2$.

Lemma 9 ([32]). *The canonical splitting fulfills*

$$\|W\|_2^2 = \|W_s\|_2^2 + \|W_r\|_2^2 \quad \text{and} \quad \|W_s\|_E^2 = \|W\|_E^2 + \|W_r\|_E^2.$$

Why is the canonical splitting interesting? The theory of statistical mechanics, applied to Euler's equations on \mathbb{S}^2 , predicts a long-time behavior of small scale fluctuations about a large scale, steady state [15]. Thus, we expect $W_r = W - W_s$ to decrease³ with time in the energy norm, which is in-sensitive to small scales. Indeed, in numerical simulations the component W_s favors evolution into large scales, while W_r favors small scales (see Fig. 5 and [32, fig. 3b]). This canonical separation of scales is a perspective on Kraichnan's [26] backward energy and forward enstrophy cascades.

³But due to Poincaré recurrence only in a statistical sense: see [zeitlin-reversibility-blog](#) [29].

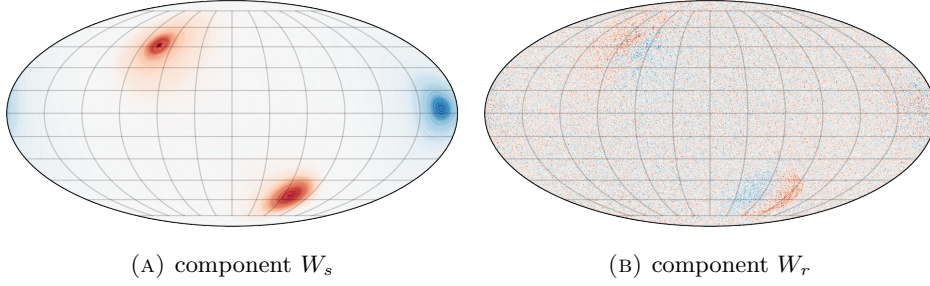


FIGURE 5. Canonical splitting $W = W_s + W_r$ of the long-time state W from Fig. 1c. The components capture the large and small scales. The projection $W \mapsto W_s$ is a mixing operator.

The canonical splitting came naturally from matrix Lie theory via the stabilizer. We now carry over the developments from $\mathfrak{su}(N)$ to $L^\infty(\mathbb{S}^2)$, which gives a connection to *mixing operators* studied by Shnirelman [34]. They are the bistochastic operators, defined in terms of kernels as

$$\mathcal{K} = \{k: \mathbb{S}^2 \times \mathbb{S}^2 \rightarrow \mathbb{R} \mid k \geq 0, \int_{\mathbb{S}^2} k(x, \cdot) = \int_{\mathbb{S}^2} k(\cdot, y) = 1\}.$$

Given $\omega, \omega' \in \overline{\mathcal{O}(\omega_0)}^* \cap \{H(\omega) = H(\omega_0)\}$, the partial ordering $\omega' \preceq \omega$ means there exists $K \in \mathcal{K}$ such that $\omega' = K\omega$. Shnirelman defines ω^* as a *minimal flow* if $\omega \preceq \omega^*$ implies $\omega^* \preceq \omega$, and he proves that such ω^* has the stationary property $\omega^* = f \circ \psi^*$ for a bounded, monotone function f .

The analog of Π_P is the operator Π_ψ for L^2 projection onto $\text{stab}_\psi = \overline{\ker\{\psi, \cdot\}}^{L^2}$, formally given by averaging along the level-sets of ψ . For a generic $\psi \in C^1(\mathbb{S}^2)$, it is well-defined as a norm-1 operator $\Pi_\psi: L^p(\mathbb{S}^2) \rightarrow L^p(\mathbb{S}^2)$ [32, prop. 5.4].

Lemma 10 ([32]). Π_ψ is a mixing operator.

In the canonical splitting $\omega = \omega_s + \omega_r$, the observed numerical decay of the energy norm $\|\omega_r\|_E^2 = \langle \omega_r, \Delta^{-1}\omega_r \rangle_{L^2}$ is compatible with Shnirelman's weak-* convergence:

Proposition 11. Let $\omega(t) \in L^\infty(\mathbb{S}^2)$ be a global solution of (5) and consider its canonical splitting $\omega(t) = \omega_s(t) + \omega_r(t)$. Then $\|\omega_r(t_n)\|_E \rightarrow 0$ if and only if $\omega_r(t_n) \xrightarrow{*} 0$ as $t_n \rightarrow \infty$.

Lemma 12. Let $\{\omega_n\}$ be a uniformly bounded sequence in L^∞ . Then $\|\omega_n - \bar{\omega}\|_{-1} \rightarrow 0$ if and only if $\omega_n \xrightarrow{*} \bar{\omega}$ weakly-* in L^∞ if and only if $\omega_n \rightharpoonup \bar{\omega}$ weakly in L^2 , for $n \rightarrow \infty$.

Proof. Weak-* convergence in L^∞ clearly implies weak convergence in L^2 , being $L^2 \subset L^1$, for bounded domains.

On the other hand, if $\omega_n \rightharpoonup \bar{\omega}$ weakly in L^2 , then being L^2 compactly embedded in H^{-1} by the Rellich–Kondrachov theorem, we have that $\|\omega_n - \bar{\omega}\|_{-1} \rightarrow 0$.

Finally, it remains to prove that convergence in H^{-1} implies convergence in the weak-* topology. Let $\phi \in C^1$, then we have that

$$\left| \int (\omega_n - \bar{\omega})\phi dS \right| \leq \|\omega_n - \bar{\omega}\|_{-1} \|\phi\|_1 \rightarrow 0, \text{ for } n \rightarrow \infty,$$

and, by hypothesis,

$$\|\omega_n - \bar{\omega}\|_\infty \leq C,$$

for any $n \geq 1$. Hence, since C^1 is dense in L^1 and the sequence of linear functionals $f_n(\phi) := \int (\omega_n - \bar{\omega})\phi dS$ defined on L^1 is bounded in norm by the constant C and so they are equicontinuous on L^1 , we get that $\omega_n \xrightarrow{*} \bar{\omega}$, for $n \rightarrow \infty$. \square

Proof of Proposition 11. The thesis follows immediately from Lemma 12 and from the uniform bound

$$\|\omega_r(t_n)\|_\infty \leq \|\omega(0)\|_\infty,$$

for any $n \geq 1$. \square

Hence, the states ω_s , observed in our long-time numerical simulations, are natural candidates for the weak-* vorticity limits. We notice that minimal flows seem too restrictive as candidates for long-time asymptotics on \mathbb{S}^2 ; essentially, they allow only two vortex condensates, or the shape of similar signed condensates would have to balance perfectly, which is physically unlikely and numerically unseen. Instead, it is common to see *branching* in the functional dependence between vorticity and stream function [32, fig. 7 and 8].

The canonical splitting offers a remedy: a selection criterion for a subset of mixing operators to define less restrictive minimal flows, namely

$$\begin{aligned} \mathcal{K}_\Pi = \{ \Pi_\psi \mid \Delta\psi \in \overline{\mathcal{O}(\omega_0)}^* \cap \{H(\Delta\psi) = H(\omega_0)\} \\ \cap \{M(\Delta\psi) = M(\omega_0)\} \}, \end{aligned}$$

where M is the angular momentum. We then expect, up to a global rotation, weak-* limits of the Euler equations as

$$\Pi_{\psi(t_n)}\omega(t_n) \xrightarrow{*} \bar{\omega}, \quad n \rightarrow \infty.$$

6. A CONJECTURE ON THE LONG-TIME BEHAVIOR AND INTEGRABILITY

One way to approach the asymptotic, long-time behavior is to ask what is contained in the ω -limit set

$$\Omega_+(\omega_0) = \bigcap_{s \geq 0} \overline{\{S_t(\omega_0) \mid t \geq s\}}^*. \quad (9)$$

Shnirelman [35] conjectured that $\Omega_+(\omega_0)$ is compact in L^2 . This conjecture can be understood as follows. $\Omega_+(\omega_0)$ is indeed compact in the weak L^2 topology, so the L^2 norm (enstrophy) attains a minimum on it, denoted by $\hat{\omega}$. We observe that $\overline{\{S_t(\hat{\omega}) \mid t \geq 0\}}^* \subset \Omega_+(\omega_0)$ and also the L^2 norm is constant on $\overline{\{S_t(\hat{\omega}) \mid t \geq 0\}}^*$. Therefore, any weakly convergent sequence in $\overline{\{S_t(\hat{\omega}) \mid t \geq 0\}}^*$ is also strongly convergent in L^2 . Consequently, the conjecture of Shnirelman is that no further mixing (loss of enstrophy) can occur for initial data in $\Omega_+(\omega_0)$.

The conjecture does not imply that steady state is reached (e.g. a minimal flow). Indeed, unsteadiness can persist indefinitely, without further mixing. From batches of numerical experiments [30], we conjecture that persistent unsteadiness in $\Omega_+(\omega_0)$ is connected to integrable configuration of “vortex blob dynamics”, where the centers of mass of n fixed-shape blobs interact (cf. Fig. 5a). Depending on the domain’s geometry, there is a threshold n for which the dynamics is always integrable [31]. The underlying mechanism is then that vortex mixing continues until a large-scale almost integrable configuration of vortex blobs is reached. Being quasi-periodic,

it then acts as a barrier for further mixing, trapping the vorticity in persistent unsteadiness. On \mathbb{S}^2 , the thresholds are $n = 3$ for generic initial data, and $n = 4$ for vanishing angular momentum. Long-time numerical simulations with Zeitlin's model align with this conjecture: for generic (smooth) initial data they typically settle on $n = 3$ blobs (e.g. Fig. 1), and for vanishing momentum on $n = 4$ blobs; see [30, Sec. 4] for details.

APPENDIX A. PROOF OF THEOREM 4

Let T_N denotes the projection of a function from $L^2(\mathbb{S}^2)$ to $\mathfrak{su}(N)$. In these calculations, we mainly follow the approach of Gallagher [13] and the results in [12, Appendix A]. We begin with the following result (with the convention that $\|\cdot\|_s$ denotes the $H^s(\mathbb{S}^2)$ Sobolev norm).

Lemma 13 (L^2 -bracket convergence). *Let $f \in H^2(\mathbb{S}^2)$ and $g \in H^6(\mathbb{S}^2)$, we have that for some $\varepsilon > 0$, $0 < \alpha < 1/2$ and $0 < \beta < 1/3$:*

$$\begin{aligned} \|[T_N \Delta^{-1} f, T_N g]_N - T_N \{\Delta^{-1} f, g\}\|_0 &\leq \frac{C(\alpha)}{N^{2-3\alpha}} \|f\|_0 \|g\|_0 \\ &+ \frac{C(\beta)}{N^{2-5\beta}} \|f\|_{-2} \|g\|_0 + \frac{C(\alpha, \varepsilon)}{N^{\alpha\varepsilon}} \|f\|_2 \|g\|_0 + \frac{C(\beta, \varepsilon)}{N^{\beta\varepsilon}} \|f\|_{-2} \|g\|_6. \end{aligned}$$

Proof. Let N be an even integer, then we want to estimate the difference:

$$\begin{aligned} \|[T_N \Delta^{-1} f, T_N g]_N - T_N \{\Delta^{-1} f, g\}\|_0^2 &= \\ &\sum_{\substack{l_1 < N, l_2 < N \\ m_1 = -l_1 : l_1 \\ m_2 = -l_2 : l_2}}^{\min\{N, l_1 + l_2 - 1\}} \sum_{\substack{l_3 = |l_1 - l_2| + 1 \\ m_3 = -l_3 : l_3}} |C_{l_1 m_1, l_2 m_2}^{l_3 m_3} - C_{l_1 m_1, l_2 m_2}^{l_3 m_3}|^2 \left| \frac{f_{l_1 m_1}}{l_1(l_1 + 1)} g_{l_2 m_2} \right|^2 = \\ &\sum_{\substack{l_1 < N^\alpha \\ l_2 < N^\beta \\ m_1 = -l_1 : l_1 \\ m_2 = -l_2 : l_2}}^{\min\{N, l_1 + l_2 - 1\}} \sum_{\substack{l_3 = |l_1 - l_2| + 1 \\ m_3 = -l_3 : l_3}} |C_{l_1 m_1, l_2 m_2}^{(N) l_3 m_3} - C_{l_1 m_1, l_2 m_2}^{l_3 m_3}|^2 \left| \frac{f_{l_1 m_1}}{l_1(l_1 + 1)} g_{l_2 m_2} \right|^2 + \\ &\sum_{\substack{N^\alpha \leq l_1 < N \\ l_2 < N^\beta \\ m_1 = -l_1 : l_1 \\ m_2 = -l_2 : l_2}}^{\min\{N, l_1 + l_2 - 1\}} \sum_{\substack{l_3 = |l_1 - l_2| + 1 \\ m_3 = -l_3 : l_3}} |C_{l_1 m_1, l_2 m_2}^{(N) l_3 m_3} - C_{l_1 m_1, l_2 m_2}^{l_3 m_3}|^2 \left| \frac{f_{l_1 m_1}}{l_1(l_1 + 1)} g_{l_2 m_2} \right|^2 + \\ &\sum_{\substack{l_1 < N^\alpha \\ N^\beta \leq l_2 < N \\ m_1 = -l_1 : l_1 \\ m_2 = -l_2 : l_2}}^{\min\{N, l_1 + l_2 - 1\}} \sum_{\substack{l_3 = |l_1 - l_2| + 1 \\ m_3 = -l_3 : l_3}} |C_{l_1 m_1, l_2 m_2}^{(N) l_3 m_3} - C_{l_1 m_1, l_2 m_2}^{l_3 m_3}|^2 \left| \frac{f_{l_1 m_1}}{l_1(l_1 + 1)} g_{l_2 m_2} \right|^2 + \\ &\sum_{\substack{N^\alpha \leq l_1 \leq N \\ N^\beta \leq l_2 < N \\ m_1 = -l_1 : l_1 \\ m_2 = -l_2 : l_2}}^{\min\{N, l_1 + l_2 - 1\}} \sum_{\substack{l_3 = |l_1 - l_2| + 1 \\ m_3 = -l_3 : l_3}} |C_{l_1 m_1, l_2 m_2}^{(N) l_3 m_3} - C_{l_1 m_1, l_2 m_2}^{l_3 m_3}|^2 \left| \frac{f_{l_1 m_1}}{l_1(l_1 + 1)} g_{l_2 m_2} \right|^2, \end{aligned}$$

where $0 < \alpha, \beta < 1$ have to be determined.

Step 1. For the first term, we have to divide sum in two cases: $l_2 < l_1 \wedge N^\beta$ and $l_1 \leq l_2 \wedge N^\alpha$. Using [12, Prop.14 (1)], we get

$$\begin{aligned}
& \sum_{\substack{l_1 < N^\alpha \\ l_2 < l_1 \wedge N^\beta \\ m_1 = -l_1:l_1 \\ m_2 = -l_2:l_2}} \sum_{\substack{\min\{N, l_1+l_2-1\} \\ l_3 = |l_1-l_2|+1 \\ m_3 = -l_3:l_3}} |C_{l_1 m_1, l_2 m_2}^{(N) l_3 m_3} - C_{l_1 m_1, l_2 m_2}^{l_3 m_3}|^2 \left| \frac{f_{l_1 m_1}}{l_1(l_1+1)} g_{l_2 m_2} \right|^2 \\
& \leq \frac{C}{N^4} \sum_{\substack{l_1 < N^\alpha \\ m_1 = -l_1:l_1}} \sum_{\substack{l_2 < l_1 \\ m_2 = -l_2:l_2}} \sum_{\substack{\min\{N, l_1+l_2-1\} \\ l_3 = |l_1-l_2|+1 \\ m_3 = -l_3:l_3}} l_1^8 \left| \frac{f_{l_1 m_1}}{l_1(l_1+1)} g_{l_2 m_2} \right|^2 \\
& \leq \frac{C}{N^4} \sum_{\substack{l_1 < N^\alpha \\ m_1 = -l_1:l_1}} \sum_{\substack{l_2 < l_1 \\ m_2 = -l_2:l_2}} l_1^6 |f_{l_1 m_1} g_{l_2 m_2}|^2 \\
& \leq \frac{C}{N^4} \left(\sum_{\substack{l_1 < N^\alpha \\ m_1 = -l_1:l_1}} l_1^3 |f_{l_1 m_1}| \right)^2 \|g\|_0^2 \\
& \leq \frac{C}{N^4} \sum_{l_1 < N^\alpha} l_1^{2\eta+1} \|f\|_{3-\eta}^2 \|g\|_0^2 \\
& \leq CN^{2\alpha(\eta+1)-4} \|f\|_{3-\eta}^2 \|g\|_0^2,
\end{aligned}$$

where we have used the the Cauchy-Schwarz inequality and the Young inequality for ℓ^p spaces. Hence, choosing $\eta = 3$, we get that we can take $\alpha < 1/2$ and the best bound is:

$$CN^{4(2\alpha-1)} \|f\|_0^2 \|g\|_0^2.$$

For the case $l_1 \leq l_2 \wedge N^\alpha$, we proceed analogously:

$$\begin{aligned}
& \frac{C}{N^4} \sum_{\substack{l_2 < N^\beta \\ l_1 \leq l_2 \wedge N^\alpha \\ m_1 = -l_1:l_1 \\ m_2 = -l_2:l_2}} \sum_{\substack{\min\{N, l_1+l_2-1\} \\ l_3 = |l_1-l_2|+1 \\ m_3 = -l_3:l_3}} l_2^8 \left| \frac{f_{l_1 m_1}}{l_1(l_1+1)} g_{l_2 m_2} \right|^2 \\
& \leq \frac{C}{N^4} \sum_{\substack{l_2 < N^\beta \\ m_2 = -l_2:l_2}} \sum_{\substack{l_1 \leq l_2 \\ m_1 = -l_1:l_1}} l_2^{10} \left| \frac{f_{l_1 m_1}}{l_1(l_1+1)} g_{l_2 m_2} \right|^2 \\
& \leq \frac{C}{N^4} \left(\sum_{\substack{l_2 < N^\beta \\ m_2 = -l_2:l_2}} l_2^5 |g_{l_2 m_2}| \right)^2 \|f\|_{-2}^2 \\
& \leq \frac{C}{N^2} \sum_{l_2 < N^\beta} l_2^{2\eta+1} \|g\|_{5-\eta}^2 \|f\|_{-2}^2 \\
& \leq CN^{2\beta(\eta+1)-4} \|g\|_{5-\eta}^2 \|f\|_{-2}^2.
\end{aligned}$$

Hence, choosing $\eta = 5$, we get that we can take $\beta < 1/3$ and the bound is:

$$CN^{4(3\beta-1)} \|f\|_{-2}^2 \|g\|_0^2.$$

Therefore, we have that the first term is bounded by:

$$\begin{aligned} & \sum_{\substack{l_1 < N^\alpha \\ l_2 < N^\beta \\ m_1 = -l_1:l_1 \\ m_2 = -l_2:l_2}} \sum_{\substack{l_3 = \min\{N, \\ l_1+l_2-1\} \\ |l_1-l_2|+1 \\ m_3 = -l_3:l_3}} |C_{l_1 m_1, l_2 m_2}^{(N) l_3 m_3} - C_{l_1 m_1, l_2 m_2}^{l_3 m_3}|^2 \left| \frac{f_{l_1 m_1}}{l_1(l_1+1)} g_{l_2 m_2} \right|^2 \\ & \leq \frac{C(\alpha)}{N^{4(1-2\alpha)}} \|f\|_0^2 \|g\|_0^2 + \frac{C(\beta)}{N^{4(1-3\beta)}} \|f\|_{-2}^2 \|g\|_0^2, \end{aligned}$$

for any $\alpha < 1/2$, $\beta < 1/3$.

Step 2. For the second term, we proceed analogously, using the result in [12, Prop.14 (2)]. Since, $\beta < \alpha$, we always have $l_2 < l_1$. Therefore,

$$\begin{aligned} & \sum_{\substack{N^\alpha < l_1 < N \\ l_2 < N^\beta \\ m_1 = -l_1:l_1 \\ m_2 = -l_2:l_2}} \sum_{\substack{l_3 = \min\{N, \\ l_1+l_2-1\} \\ |l_1-l_2|+1 \\ m_3 = -l_3:l_3}} |C_{l_1 m_1, l_2 m_2}^{(N) l_3 m_3} - C_{l_1 m_1, l_2 m_2}^{l_3 m_3}|^2 \left| \frac{f_{l_1 m_1}}{l_1(l_1+1)} g_{l_2 m_2} \right|^2 \\ & \leq C \sum_{\substack{N^\alpha < l_1 < N \\ m_1 = -l_1:l_1}} \sum_{\substack{l_2 < N^\beta \\ m_2 = -l_2:l_2}} \sum_{\substack{l_3 = |l_1-l_2|+1 \\ m_3 = -l_3:l_3}}^{\min\{N, l_1+l_2-1\}} l_1^4 \left| \frac{f_{l_1 m_1}}{l_1(l_1+1)} g_{l_2 m_2} \right|^2 \\ & \leq C \sum_{\substack{N^\alpha < l_1 < N \\ m_1 = -l_1:l_1}} \sum_{\substack{l_2 < N^\beta \\ m_2 = -l_2:l_2}} l_1^2 |f_{l_1 m_1} g_{l_2 m_2}|^2 \\ & \leq C \sum_{\substack{N^\alpha < l_1 < N \\ m_1 = -l_1:l_1}} l_1^2 |f_{l_1 m_1}|^2 \|g\|_0^2 \\ & \leq C \sum_{\substack{N^\alpha < l_1 < N \\ m_1 = -l_1:l_1}} |f_{l_1 m_1}|^2 \|f\|_2^2 \|g\|_0^2 \\ & \leq CN^{-2\alpha\varepsilon} \|f\|_2^2 \|g\|_0^2, \end{aligned}$$

where we have used the fact that $\sum_{m_1 = -l_1:l_1} |f_{l_1 m_1}|^2 \sim l_1^{-1-2\varepsilon}$, for some $\varepsilon > 0$.

Therefore, we have that the second term is bounded by:

$$\begin{aligned} & \sum_{\substack{N^\alpha < l_1 < N \\ l_2 < N^\beta \\ m_1 = -l_1:l_1 \\ m_2 = -l_2:l_2}} \sum_{\substack{l_3 = \min\{N, \\ l_1+l_2-1\} \\ |l_1-l_2|+1 \\ m_3 = -l_3:l_3}} |C_{l_1 m_1, l_2 m_2}^{(N) l_3 m_3} - C_{l_1 m_1, l_2 m_2}^{l_3 m_3}|^2 \left| \frac{f_{l_1 m_1}}{l_1(l_1+1)} g_{l_2 m_2} \right|^2 \\ & \leq \frac{C(\alpha, \varepsilon)}{N^{2\alpha\varepsilon}} \|f\|_2^2 \|g\|_0^2, \end{aligned}$$

for any $\alpha < 1/2$, $\beta < 1/3$ and some $\varepsilon > 0$.

Step 3. For the third term, we proceed by dividing the cases for which $l_2 < l_1$ and $l_1 \leq l_2 \wedge N^\alpha$. When $l_2 < l_1$, we can repeat the same calculations of Step 1,

getting the same bound. When $l_1 \leq l_2 \wedge N^\alpha$, we consider

$$\begin{aligned}
& \sum_{\substack{N^\beta < l_2 < N \\ l_1 \leq l_2 \wedge N^\alpha \\ m_2 = -l_2 : l_2 \\ m_1 = -l_1 : l_1}} \sum_{\substack{\min\{N, l_1 + l_2 - 1\} \\ l_3 = |l_1 - l_2| + 1 \\ m_3 = -l_3 : l_3}} |C_{l_1 m_1, l_2 m_2}^{(N) l_3 m_3} - C_{l_1 m_1, l_2 m_2}^{l_3 m_3}|^2 \left| \frac{f_{l_1 m_1}}{l_1(l_1 + 1)} g_{l_2 m_2} \right|^2 \\
& \leq C \sum_{\substack{N^\beta < l_2 < N \\ m_2 = -l_2 : l_2}} \sum_{\substack{l_1 < l_2 \\ m_1 = -l_1 : l_1}} \sum_{\substack{\min\{N, l_1 + l_2 - 1\} \\ l_3 = |l_1 - l_2| + 1 \\ m_3 = -l_3 : l_3}} l_2^4 \left| \frac{f_{l_1 m_1}}{l_1(l_1 + 1)} g_{l_2 m_2} \right|^2 \\
& \leq C \sum_{\substack{N^\beta < l_2 < N \\ m_2 = -l_2 : l_2}} l_2^6 |g_{l_2 m_2}|^2 \|f\|_{-2}^2 \\
& \leq C \sum_{\substack{N^\beta < l_2 < N \\ m_2 = -l_2 : l_2}} |g_{l_2 m_2}|^2 \|f\|_{-2}^2 \|g\|_6^2 \\
& \leq C N^{-2\beta\varepsilon} \|f\|_{-2}^2 \|g\|_6^2,
\end{aligned}$$

where we have used the fact that $\sum_{m_2 = -l_2 : l_2} |g_{l_2 m_2}|^2 \sim l_2^{-1-2\varepsilon}$, for some $\varepsilon > 0$.

Therefore, we have that the third term is bounded by:

$$\begin{aligned}
& \sum_{\substack{l_1 < N^\alpha \\ N^\beta < l_2 < N \\ m_2 = -l_2 : l_2 \\ m_1 = -l_1 : l_1}} \sum_{\substack{\min\{N, l_1 + l_2 - 1\} \\ l_3 = |l_1 - l_2| + 1 \\ m_3 = -l_3 : l_3}} |C_{l_1 m_1, l_2 m_2}^{(N) l_3 m_3} - C_{l_1 m_1, l_2 m_2}^{l_3 m_3}|^2 \left| \frac{f_{l_1 m_1}}{l_1(l_1 + 1)} g_{l_2 m_2} \right|^2 \\
& \leq \frac{C(\alpha)}{N^{4(1-2\alpha)}} \|f\|_0^2 \|g\|_0^2 + \frac{C(\beta, \varepsilon)}{N^{2\beta\varepsilon}} \|f\|_{-2}^2 \|g\|_6^2,
\end{aligned}$$

for any $\alpha < 1/2$, $\beta < 1/3$ and some $\varepsilon > 0$.

Step 4. For the third term, we proceed by dividing the cases for which $l_2 < l_1$ and $l_1 \leq l_2$. In either case, we get the same bound obtained in Step 2 and 3, respectively.

Therefore, we have that the fourth term is bounded by:

$$\begin{aligned}
& \sum_{\substack{N^\alpha \leq l_1 \leq N \\ N^\beta \leq l_2 < N \\ m_1 = -l_1 : l_1 \\ m_2 = -l_2 : l_2}} \sum_{\substack{\min\{N, l_1 + l_2 - 1\} \\ l_3 = |l_1 - l_2| + 1 \\ m_3 = -l_3 : l_3}} |C_{l_1 m_1, l_2 m_2}^{(N) l_3 m_3} - C_{l_1 m_1, l_2 m_2}^{l_3 m_3}|^2 \left| \frac{f_{l_1 m_1}}{l_1(l_1 + 1)} g_{l_2 m_2} \right|^2 \\
& \leq \frac{C(\alpha, \varepsilon)}{N^{2\alpha\varepsilon}} \|f\|_2^2 \|g\|_0^2 + \frac{C(\beta, \varepsilon)}{N^{2\beta\varepsilon}} \|f\|_{-2}^2 \|g\|_6^2,
\end{aligned}$$

for any $\alpha < 1/2$, $\beta < 1/3$ and some $\varepsilon > 0$. □

We can now state the L^2 convergence of the quantized bracket to the original one.

Corollary 14 (Spatial convergence). *In the framework of Lemma 13, we have that:*

$$\|T_N^* [T_N \Delta^{-1} f, T_N g]_N - \{\Delta^{-1} f, g\}\|_0 \leq \frac{C(\alpha)}{N^{2-3\alpha}} \|f\|_0 \|g\|_0$$

$$+ \frac{C(\beta)}{N^{2-5\beta}} \|f\|_{-2} \|g\|_0 + \frac{C(\alpha)}{N^{\alpha\varepsilon}} \|f\|_2 \|g\|_0 + \frac{C(\beta)}{N^{\beta\varepsilon}} \|f\|_{-2} \|g\|_6,$$

for some $\varepsilon > 0$, $0 < \alpha < 1/2$ and $0 < \beta < 1/3$.

Proof. We have that:

$$\begin{aligned} & \|T_N^*[T_N\Delta^{-1}f, T_Ng]_N - \{\Delta^{-1}f, g\}\|_0 \\ &= \| [T_N\Delta^{-1}f, T_Ng]_N - T_N\{\Delta^{-1}f, g\} \|_0 + \|(Id - T_N^*T_N)\{\Delta^{-1}f, g\}\|_0. \end{aligned}$$

The first term has been estimate in Lemma 13, so we have to study only the residual term

$$\begin{aligned} & \|(Id - T_N^*T_N)\{\Delta^{-1}f, g\}\|_0^2 = \\ & \sum_{\substack{l_1 > N \\ m_1 = -l_1 : l_1}} \sum_{\substack{l_2 > N \\ m_2 = -l_2 : l_2}} \sum_{\substack{l_1+l_2-1 \\ l_3=|l_1-l_2|+1 \\ m_3=-l_3:l_3}} |C_{l_1 m_1, l_2 m_2}^{l_3 m_3}|^2 \left| \frac{f_{l_1 m_1}}{l_1(l_1+1)} g_{l_2 m_2} \right|^2. \end{aligned}$$

Repeating the same calculations of Lemma 13, Step 4, and using the result in [12, Lemma 12], we get that:

$$\begin{aligned} & \sum_{\substack{l_1 > N \\ m_1 = -l_1 : l_1}} \sum_{\substack{l_2 > N \\ m_2 = -l_2 : l_2}} \sum_{\substack{l_1+l_2-1 \\ l_3=|l_1-l_2|+1 \\ m_3=-l_3:l_3}} |C_{l_1 m_1, l_2 m_2}^{l_3 m_3}|^2 \left| \frac{f_{l_1 m_1}}{l_1(l_1+1)} g_{l_2 m_2} \right|^2 \\ & \leq \frac{C(\alpha)}{N^{2\varepsilon}} \|f\|_2^2 \|g\|_0^2 + \frac{C(\beta)}{N^{2\varepsilon}} \|f\|_{-2}^2 \|g\|_6^2, \end{aligned}$$

for some $\varepsilon > 0$. Hence, the residual term $\|(Id - T_N^*T_N)\{\Delta^{-1}f, g\}\|_0$ does not worsen the bound of Lemma 13. \square

The last ingredient we need for the proof of the convergence is the following:

Lemma 15. *In the above framework*

$$\|T_N\{\Delta^{-1}f, g\}\|_0 \leq C \|f\|_{-1} \|\nabla g\|_\infty.$$

Proof. We have that

$$\begin{aligned} \|T_N\{\Delta^{-1}f, g\}\|_0 & \leq \|\{\Delta^{-1}f, g\}\|_0 \\ & = \left(\int |\nabla \Delta^{-1}f \times \nabla g|^2 \right)^{1/2} \\ & \leq C \left(\int |\nabla \Delta^{-1}f|^2 \right)^{1/2} \|\nabla g\|_\infty \\ & \leq C \|f\|_{-1} \|\nabla g\|_\infty. \end{aligned}$$

\square

Theorem 16 (Space-time convergence). *Let ω and W be respectively the solutions to the Euler 5 and quantized Euler equations 7, with initial data, respectively, $\omega(0) \in H^6(\mathbb{S}^2)$ and $W(0) \in \mathfrak{su}(N)$. Let $\omega_N(t) := T_N^*W(t)$, for any $t \geq 0$. We have that:*

$$\begin{aligned} \|\omega(t) - \omega_N(t)\|_0 & \leq C \left(\|\omega(0) - \omega_N(0)\|_0 + \right. \\ & \left. \frac{C(\alpha)}{N^{2(1-2\alpha)}} \|\omega(0)\|_0^2 t + \frac{C(\beta)}{N^{2(1-3\beta)}} \|\omega(0)\|_0^2 t + \right. \end{aligned}$$

$$\begin{aligned} & \frac{C(\alpha)}{N^{\alpha\varepsilon}} \|\omega(0)\|_0 \int_0^t \|\omega(s)\|_2 ds + \frac{C(\beta)}{N^{\beta\varepsilon}} \|\omega(0)\|_0 \int_0^t \|\omega(s)\|_6 ds \Big) \cdot \\ & \exp \left\{ C \int_0^t \frac{C(\alpha)}{N^{2(1-2\alpha)}} \|\omega(s)\|_0 + \frac{C(\beta)}{N^{2(1-3\beta)}} \|\omega(s)\|_0 + \right. \\ & \left. \|\nabla\omega(s)\|_\infty ds \right\}, \end{aligned}$$

for any $t \geq 0$ and for some $\varepsilon > 0$, $0 < \alpha < 1/2$ and $0 < \beta < 1/3$.

Proof. Following [13], we consider:

$$\begin{aligned} & \frac{1}{2} \frac{d}{dt} \|\omega_N(t) - \omega(t)\|_0^2 = \\ & = \langle \omega_N(t) - \omega(t), T_N^* [\Delta_N^{-1} W(t), W(t)]_N - \{\Delta^{-1} \omega(t), \omega(t)\} \rangle. \end{aligned} \quad (10)$$

By the definition of the bracket, we get that:

$$0 = \langle \omega_N(t) - \omega(t), T_N^* [\Delta_N^{-1} W(t), W(t) - T_N \omega(t)]_N \rangle,$$

therefore equation (10) can be written as:

$$\begin{aligned} & \frac{1}{2} \frac{d}{dt} \|\omega_N(t) - \omega(t)\|_0^2 = \\ & = \langle \omega_N(t) - \omega(t), T_N^* [\Delta_N^{-1} W(t), T_N \omega(t)]_N - \{\Delta^{-1} \omega(t), \omega(t)\} \rangle \\ & = \langle \omega_N(t) - \omega(t), T_N^* [\Delta_N^{-1} T_N \omega(t), T_N \omega(t)]_N - \{\Delta^{-1} \omega(t), \omega(t)\} \rangle \\ & + \langle \omega_N(t) - \omega(t), T_N^* [\Delta_N^{-1} (W(t) - T_N \omega(t)), T_N \omega(t)]_N \rangle. \end{aligned}$$

The second term on the RHS can be written as

$$\begin{aligned} & \langle \omega_N(t) - \omega(t), T_N^* [\Delta_N^{-1} (W(t) - T_N \omega(t)), T_N \omega(t)]_N \rangle = \\ & = \langle \omega_N(t) - \omega(t), T_N^* ([\Delta_N^{-1} (W(t) - T_N \omega(t)), T_N \omega(t)]_N \\ & - T_N \{\Delta^{-1} (\omega_N(t) - T_N \omega(t)), T_N \omega(t)\}) \rangle \\ & + \langle \omega_N(t) - \omega(t), T_N^* T_N \{\Delta^{-1} (\omega_N(t) - T_N \omega(t)), T_N \omega(t)\} \rangle \end{aligned}$$

From Lemma 13, Corollary 14 and Lemma 15, we can then deduce that:

$$\begin{aligned} & \frac{1}{2} \frac{d}{dt} \|\omega_N(t) - \omega(t)\|_0^2 \leq C \|\omega_N(t) - \omega(t)\|_0 \|\omega(t)\|_0 \cdot \\ & \left(\frac{C(\alpha)}{N^{2(1-2\alpha)}} \|\omega(t)\|_0 + \frac{C(\beta)}{N^{2(1-3\beta)}} \|\omega(t)\|_0 + \right. \\ & \left. \frac{C(\alpha)}{N^{\alpha\varepsilon}} \|\omega(t)\|_2 + \frac{C(\beta)}{N^{\beta\varepsilon}} \|\omega(t)\|_6 \right) + \\ & C \|\omega_N(t) - \omega(t)\|_0^2 \cdot \\ & \left(\frac{C(\alpha)}{N^{2(1-2\alpha)}} \|\omega(t)\|_0 + \frac{C(\beta)}{N^{2(1-3\beta)}} \|\omega(t)\|_0 + \|\nabla\omega\|_\infty \right). \end{aligned}$$

The thesis then follows from the Grönwall lemma. \square

REFERENCES

- [1] R. V. Abramov and A. J. Majda, Statistically relevant conserved quantities for truncated quasigeostrophic flow, *Proc. Natl. Acad. Sci. USA* **100** (2003), 3841–3846.

- [2] E. Caglioti, P. L. Lions, C. Marchioro, and M. Pulvirenti, A special class of stationary flows for two-dimensional euler equations: A statistical mechanics description, *Comm. Math. Phys.* **143** (1992), 501–525.
- [3] L. Charles and L. Polterovich, Sharp correspondence principle and quantum measurements, *St. Petersburg Math. J.* **29** (2018), 177–207.
- [4] J. Chen, T. Y. Hou, and D. Huang, On the finite time blowup of the De Gregorio model for the 3D Euler equations, *Comm. Pure Appl. Math.* **74** (2021), 1282–1350.
- [5] P. Cifani, M. Viviani, and K. Modin, An efficient geometric method for incompressible hydrodynamics on the sphere, *J. Comput. Phys.* **473** (2023), 111772.
- [6] S. De Gregorio, On a one-dimensional model for the three-dimensional vorticity equation, *J. Statist. Phys.* **59** (1990), 1251–1263.
- [7] M. Dolce and T. D. Drivas, On maximally mixed equilibria of two-dimensional perfect fluids, *Arch. Ration. Mech. Anal.* **246** (2022), 735–770.
- [8] S. K. Donaldson, Some numerical results in complex differential geometry, *Pure and Applied Mathematics Quarterly* **5** (2009), 571–618.
- [9] T. D. Drivas and T. M. Elgindi, Singularity formation in the incompressible Euler equation in finite and infinite time, *EMS Surv. Math. Sci.* **10** (2023), 1–100.
- [10] T. M. Elgindi and I.-J. Jeong, On the effects of advection and vortex stretching, *Arch. Rational Mech. Anal.* **235** (2020), 1763–1817.
- [11] L. Euler, Principes généraux de l'état d'équilibre d'un fluide, *Académie Royale des Sciences et des Belles-Lettres de Berlin, Mémoires* **11** (1757), 217–273.
- [12] F. Flandoli, U. Pappalettera, and M. Viviani, On the infinite dimension limit of invariant measures and solutions of Zeitlin's 2D Euler equations, *J. Stat. Phys.* **189** (2022).
- [13] I. Gallagher, Mathematical analysis of a structure-preserving approximation of the bidimensional vorticity equation, *Numer. Math.* **91** (2002), 223–236.
- [14] H. Helmholtz, Über integrale der hydrodynamischen gleichungen, welcher der wirbelbewegungen entsprechen, *J. Reine Angew. Math.* **55** (1858), 25–55.
- [15] C. Herbert, Additional invariants and statistical equilibria for the 2d euler equations on a spherical domain, *Journal of Statistical Physics* **152** (2013), 1084–1114.
- [16] J. Hoppe, *Quantum theory of a massless relativistic surface and a two-dimensional bound state problem*, Ph.D. thesis, Massachusetts Institute of Technology, 1982.
- [17] J. Hoppe, Diffeomorphism groups, quantization, and $SU(\infty)$, *Int. J. Modern Phys. A* **04** (1989), 5235–5248.
- [18] J. Hoppe and S.-T. Yau, Some properties of matrix harmonics on S^2 , *Comm. Math. Phys.* **195** (1998), 67–77.
- [19] A. Izosimov, B. A. Khesin, and M. Mousavi, Coadjoint orbits of symplectic diffeomorphisms of surfaces and ideal hydrodynamics, *Ann. Inst. Fourier (Grenoble)* **66** (2016), 2385–2433.
- [20] L. Kelvin, Stability of fluid motion-rectilinear motion of viscous fluid between two plates, *Philos. Mag.* **24** (1887).
- [21] B. Khesin, G. Misiolek, and A. Shnirelman, Geometric hydrodynamics in open problems, arXiv, 2022.

- [22] M. K.-H. Kiessling, Statistical mechanics of classical particles with logarithmic interactions, *Comm. Pure Appl. Math.* **46** (1993), 27–56.
- [23] G. Kirchhoff, *Vorlesungen über mathematische physik: mechanik*, BG Teubner, 1876.
- [24] A. Kiselev and V. Šverák, Small scale creation for solutions of the incompressible two-dimensional Euler equation, *Ann. of Math.* **180** (2014), 1205–1220.
- [25] A. Knapp, Group representations and harmonic analysis from euler to langlands, part ii, *Notices Amer. Math. Soc.* **43** (1996), 537–549.
- [26] R. H. Kraichnan, Inertial ranges in two-dimensional turbulence, *The Physics of Fluids* **10** (1967), 1417–1423.
- [27] E. N. Lorenz, The statistical prediction of solutions of dynamical equations, *Proceedings of the International Symposium on Numerical Weather Prediction, 1962*, 1962.
- [28] C. Marchioro and M. Pulvirenti, *Mathematical theory of incompressible non-viscous fluids*, vol. 96, Springer Science & Business Media, 2012.
- [29] K. Modin, The reversibility paradox in Zeitlin’s model, klasmodin.github.io/blog/2023/zeitlin-reversibility, 2023.
- [30] K. Modin and M. Viviani, A Casimir preserving scheme for long-time simulation of spherical ideal hydrodynamics, *J. Fluid Mech.* **884** (2020).
- [31] K. Modin and M. Viviani, Integrability of point-vortex dynamics via symplectic reduction: A survey, *Arnold Math. J.* **7** (2020).
- [32] K. Modin and M. Viviani, Canonical scale separation in 2d incompressible hydrodynamics, *J. Fluid Mech.* **943** (2022), A36.
- [33] L. Onsager, Statistical hydrodynamics, *Il Nuovo Cimento (1943-1954)* **6** (1949), 279–287.
- [34] A. Shnirelman, Lattice theory and flows of ideal incompressible fluid, *Russ. J. Math. Phys.* **1** (1993), 105–113.
- [35] A. Shnirelman, On the long time behavior of fluid flows, *Procedia IUTAM* **7** (2013), 151–160.
- [36] V. Šverák, Lecture notes on hydrodynamics, <http://www-users.math.umn.edu/~sverak/course-notes2011.pdf>, 2011.
- [37] G. Tian, On a set of polarized Kähler metrics on algebraic manifolds, *J. Differential Geom.* **32** (1990), 99–130.
- [38] Y. Wang, C.-Y. Lai, J. Gómez-Serrano, and T. Buckmaster, Asymptotic self-similar blow up profile for 3-D Euler via physics-informed neural networks, arXiv:2201.06780, 2022.
- [39] V. I. Yudovich, Non-stationary flows of an ideal incompressible fluid, *Zh. Vychisl. Mat. Mat. Fiz.* **3** (1963), 1032–1066.
- [40] V. Zeitlin, Finite-mode analogs of 2D ideal hydrodynamics: coadjoint orbits and local canonical structure, *Phys. D* **49** (1991), 353–362.
- [41] V. Zeitlin, Self-consistent finite-mode approximations for the hydrodynamics of an incompressible fluid on nonrotating and rotating spheres, *Phys. Rev. Lett.* **93** (2004), 264501.